Experimental Characterisation of Hydraulic Fiber-Reinforced Soft Actuators for Worm-Like Robots

Matheus S. Xavier, Andrew J. Fleming and Yuen K. Yong
Precision Mechatronics Lab, School of Electrical Engineering and Computing
The University of Newcastle
Callaghan, NSW 2308, Australia
{*matheus.xavier, andrew.fleming, yuenkuan.yong*}*@newcastle.edu.au*

***Abstract*— This article describes the design and fabrication of fiber-reinforced soft actuators for a worm-like robot designed to operate inside constrained tubes. The actuators include bending, extension and torsion. These actuators are experimentally characterised by measuring the deflection versus applied pressure. The results demonstrate that fiber wrapping pattern, geometry of cross-section and elastomer selection are the main determinants of performance. The actuators under consideration are employed to construct a soft worm-like robot capable of ascending a pipe. This class of applications includes steerable catheters, endoscopes and pipe inspection devices.**

***Index Terms*— Soft actuators, Fiber-reinforced actuators, Bio-inspired robotics, Worm-like robot, Biomedical devices.**

I. INTRODUCTION

Conventional robot manipulators ("vertebrate robots" or discrete robots) [1] are constructed from rigid links connected through joints with a single degree of freedom (DOF) and have been employed in many industrial applications with high speed and accuracy. These robots are very efficient for open environments but might not reach desired end-effector positions as constraints are added [2]. By increasing the number of discrete joints and making the rigid links very short, serpentine robots are achieved. Serpentine robots produce smooth curves similar to a snake [3]. Continuum robots ("invertebrate robots") [2]–[5], on the other hand, do not contain rigid links and can be defined as infinite degrees of freedom robots with elastic structures [5]. These robots can bend, extend/contract and sometimes twist at any point along their structure and produce motion through the generation of smooth curves [3], [4]. Due to their conformal deformation, they can adapt to delicate objects, lowering the number of parts required for a given task and increasing safety and dexterity [6]. Furthermore, continuum robots can be lightweight and employed within constrained environments with restricted access [2], [3].

Continuum style robots composed of highly deformable and compliant materials, such as silicone rubber, are denominated soft robots [7]–[9]. These flexible (elastomeric) materials typically exhibit large strains and low elastic moduli (Young's modulus $\sim 10^2 - 10^6$ Pa) [10]. They show high dexterity but with low accuracy and difficult motion control and sensing [8], [9]. The majority of soft robots are composed of pressure-driven actuators, the so-called soft fluidic actuators or elastic inflatable actuators [11], [12]. These actuators are driven by the deformation of a chamber or membrane with pneumatics or hydraulics. Advantages include high force densities (> 1 mN mm^{-3}) and affordability [7], [10].

Soft fluidic actuators can be classified by their motion into four categories: extending, contracting, bending and twisting. These actuators have anisotropic flexible structures to achieve each motion category [7], [13]. The simplest design for soft fluidic actuators consists of a single chamber. However, unless fibers are wrapped around the single chamber actuator, the actuator behaves as a balloon with high radial expansion [14], [15]. The most investigated design in the literature is the multi-chambered actuator. A popular example is the PneuNets [16]–[18], which consist of an extensible top layer and an inextensible but flexible bottom layer. The slow PneuNets [16], [19] are constructed from a block of silicone rubber with embedded air chambers; while the fast PneuNets [17] contain gaps between the inside walls of each chamber. Other designs for multi-chambered actuators (fast PneuNets) use trapezoidal [15] and triangular [20] bellows.

Soft actuators are commonly manufactured with the aid of additive manufacturing. In most cases, molds are 3D-printed into which silicones are cast and consolidated [21]. The use of 3D printing allows the design of complex features and high precision molds with a lower number of manufacturing steps [22], [23]. After curing the rubber, tubes are inserted for actuation. The fabrication of some actuators also include bonding fabric [19] and/or fiber reinforcements to the actuator [10].

In this article, fiber-reinforced actuators [10], [24], [25] are analysed. As shown in Fig. 1, fibers such as Kevlar can be arranged along the actuator length to achieve different motions, e.g. (a) double helical wrapping and strain limiting layer for bending; (b) double helical wrapping for extending; (c) single helical wrapping and strain limiting layer for twisting and bending; and (d) single helical wrapping for twisting and extending. Moreover, an actuator can be fabricated with different motion types in different segments, thus combining multiple behaviours.

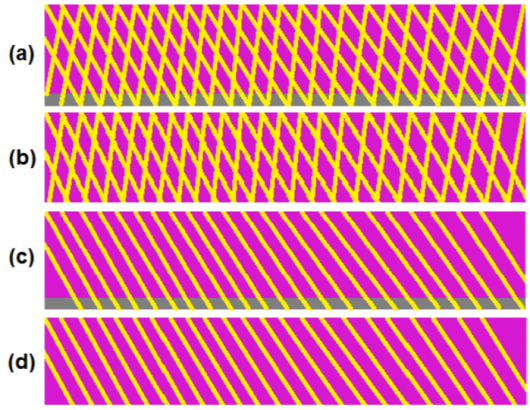

Fig. 1: Different types of fiber-reinforced actuators. (a) Bending, (b) extending, (c) twisting and bending, and (d) twisting and extending actuators. The silicone rubber is shown in magenta, the fiber wrappings in yellow and the strain limiting layer in gray.

The majority of soft actuators proposed in the literature are characterised using air [15], [17], [19]. However, hydraulic actuators are safer in biomedical applications such as steerable catheters where physiological saline can be used as a driving fluid [26], [27].

A. *Contributions of this work*

This article presents an experimental comparison of hydraulic fiber-reinforced actuators to produce bending, extending, and twisting. In the first section, the actuator behaviour and fabrication methods are described. Experimental results are then presented to demonstrate the key parameters which determine performance. Finally, the actuators are employed in an example application to construct a worm-like robot for navigating tube environments.

II. DESIGN AND FABRICATION

A. *Design*

The collection of 26 soft actuators analysed in this work are summarised in Table I. Rectangular, semi-circular and circular cross-sections are investigated. Furthermore, combinations of single actuators are used to fabricate bi-directional and parallel bellows actuators. The rectangular actuators have a fixed length of 80 mm and sides of 16 mm, while the wall thickness varied from 1 mm to 3 mm. The semi-circular actuators have a fixed length of 80 mm and diameter of 14 mm, while the thicknesses are 2 mm and 3 mm. The circular actuators have length of 90 mm, diameter of 16.7 mm and thickness of 2 mm.

B. *Fabrication*

Two types of silicone rubber are used: Elastosil M4601 (28 A hardness, tensile strength of 6.48 MPa, colour: pink) and Dragon Skin 10 (10 A hardness, tensile strength of 3.28 MPa, colour: translucent, hereafter denoted as DS10). The molds for the actuators were designed in Autodesk Inventor and are shown in Fig. 2. The molds were 3D printed using a Form 2 (Formlabs) and a MakerBot Replicator 2X (MakerBot Industries).

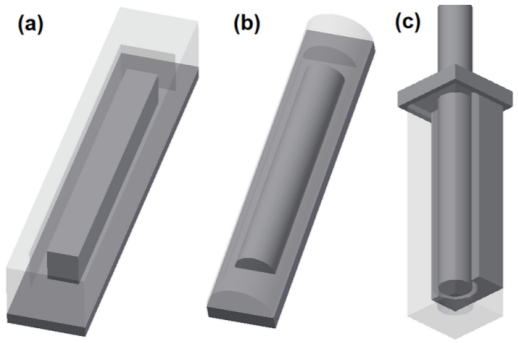

Fig. 2: 3D printed mold designs in Inventor. (a) Rectangular, (b) semi-circular, and (c) circular molds.

The following steps are followed in the fabrication of rectangular and semi-circular soft actuators [15], [21], [28]. Firstly, the silicone rubber is mixed in the recommended proportions (9:1 for M4601 and 1:1 for DS10). This mixture is degassed in a vacuum chamber and poured into the bottom half of the mold. The top half of the mold is then inserted and the mold is left for curing at room temperature. For the cylindrical actuator, the left and right molds are clamped together using rubber bands. Afterwards, the mixture is poured into the mold and the metal rod is inserted. Finally, the top cap is used to fix the rod in place and ensure uniform thickness along the length of the actuator.

After curing, the soft actuators are removed from the mold. For bending actuators, a strain limiting layer (fiberglass fab-

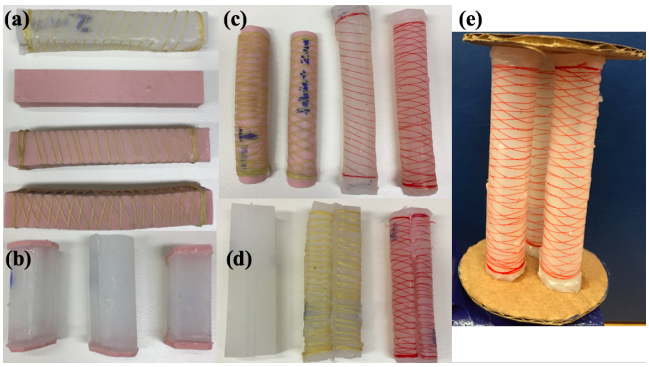

Fig. 3: Photographs of fiber-reinforced soft actuators fabricated in this work. (a) Rectangular, (b) lateral expanding, (c) semi-circular and circular, (d) bi-directional, and (e) parallel bellows actuators.

Label	Cross-section	Material	Thickness	Fiber wrap	Fabric	Motion
Actuator 1	Rectangular	Elastosil M4601	1 mm	No	Yes	Bending
Actuator 2	Rectangular	Elastosil M4601	3 mm	Double	Yes	Bending
Actuator 5	Rectangular	Elastosil M4601	3 mm	No	Yes	Bending
Actuator 6	Rectangular	M4601+DS10	2 mm	No	No	Bending
Actuator 10	Rectangular	DragonSkin 10	3 mm	Double	Yes	Bending
Actuator 11	Semi-circular	Elastosil M4601	1 mm	Double	Yes	Bending
Actuator 12	Semi-circular	Elastosil M4601	2 mm	Double	Yes	Bending
Actuator 13	Semi-circular	Elastosil M4601	2 mm	No	No	Bending
Actuator 14	Semi-circular	DragonSkin 10	2 mm	Double	Yes	Bending
Actuator 15	Bi-directional (rect)	DragonSkin 10	3 mm	No	No	Bending
Actuator 16	Bi-directional (rect)	DragonSkin 10	3 mm	Double	No	Bending
Actuator 17	Bi-directional (semi-circ)	DragonSkin 10	2 mm	Double	Yes	Bending
Actuator 18	Bi-directional (semi-circ)	DragonSkin 10	2 mm	Double	Yes	Bending
Actuator 3	Rectangular	Elastosil M4601	3 mm	Double	No	Extending
Actuator 7	Rectangular	DragonSkin 10	2 mm	Double	No	Extending
Actuator 20	Circular	DragonSkin 10	2 mm	Double	No	Extending
Actuator 4	Rectangular	Elastosil M4601	3 mm	Single	Yes	Twist/bend
Actuator 9	Rectangular	DragonSkin 10	2 mm	Single	Yes	Twist/bend
Actuator 8	Rectangular	DragonSkin 10	2 mm	Single	No	Twist/extend
Actuator 19	Circular	DragonSkin 10	2 mm	Single	No	Twist/extend
Actuator 21	PBA (unconstrained)	DragonSkin 10	2 mm	Double	No	Extend/bend
Actuator 22	PBA (constrained)	DragonSkin 10	2 mm	Double	No	Extend/bend
Actuator 23	Rectangular	M4601+DS10	2 mm	No	No	Anchoring
Actuator 24	Rectangular	M4601+DS10	2 mm	No	No	Anchoring
Actuator 25	Circular	M4601+DS10	2 mm	No	Yes	Anchoring
Actuator 26	Circular	M4601+DS10	1 mm	No	Yes	Anchoring

TABLE I: Collection of soft actuators in this work.

ric) is added to one side of the actuators (optional for semi-circular actuators). For twisting actuators, a single helical wrapping of Kevlar thread (yellow) or sewing thread (red) is performed along the length of the actuator. For extending actuators, a double helical wrapping was included in most actuators. A thin layer of DS10 is applied to secure the thread placement.

For bi-directional actuators, two rectangular or semi-circular actuators with double wrapping were glued together using silicone adhesive. For the parallel bellows actuator, three cylindrical actuators with double helical wrapping were placed along the edges of an equilateral triangle and held in position between two circular cardboard platforms. Some of the fabricated actuators are shown in Fig. 3.

During the fabrication of soft actuators, we have noticed that (a) to facilitate the manipulation of the actuators, the strain limiting layer or simply adding the silicone bottom layer should be performed before wrapping the fiber, especially for the softer rubber with smaller thicknesses; (b) a second mold should be employed to achieve uniform distribution of the DS10 layer used to maintain the thread path (a nonuniform distribution results in some level of bending); and (c) indents in the mold should be used to facilitate wrapping at specific angles and obtain a more uniform pattern. Nonuniform fiber distribution with large gaps between fiber wraps might lead to unwanted wall expansion or explosion after pressurisation.

III. ACTUATOR CHARACTERISATION

The actuators were characterised using water as a driving fluid with the actuator cantilevered vertically using a mechanical fixture. Commercially available 20 mL plastic syringes were used to input pressure. The pressure measurements were obtained using an analog water pressure sensor (SEN0257, DFRobot) connected to an Arduino Mega 2560. PLX-DAQ

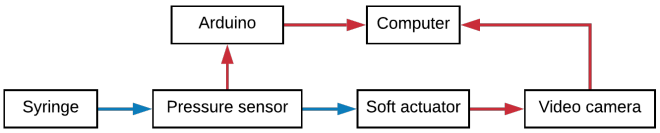

Fig. 4: Experimental setup for actuator characterisation. Blue and red arrows denote hydraulic and data lines, respectively.

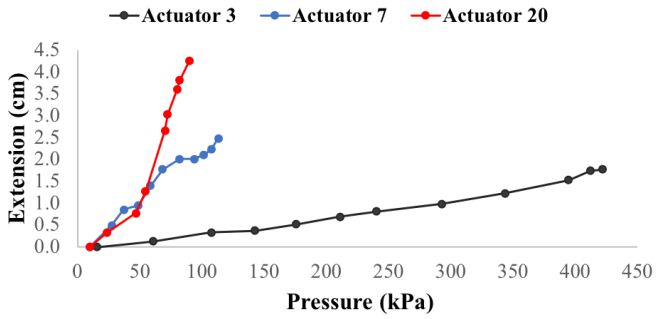

Fig. 5: Performance of selected extending actuators for a range of input pressures.

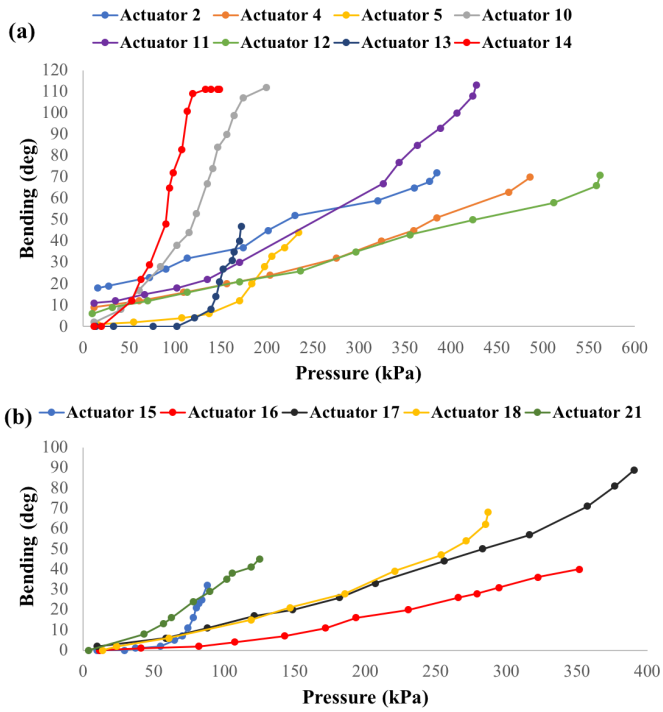

Fig. 6: Performance of selected bending actuators for a range of input pressures. (a) Bending angle of single actuators. (b) Bending angle of bi-directional and parallel bellows actuators.

was used to store the real-time pressure measurements from this system into an Excel file for further analysis. The motion of the actuators were recorded with a video camera (60 fps) and the images were post-processed using Kinovea to measure the angles and extensions.

A. *Extending actuators*

The extensions shown in Fig. 5 were measured by first calibrating the dimensions in Kinovea with respect to the known fixture side length and then measuring the length of the actuators for the respective pressure steps.

From Fig. 5, the rectangular actuator fabricated with DS10 (actuator 7) had a maximum extension 40% higher than its M4601 counterpart. Among the two extending DS10 actuators, the circular actuator achieves the highest extension of 4.25 cm at the pressure of 90 kPa, an improvement of 71% in comparison with the rectangular actuator.

B. *Bending actuators*

For the bending actuators, the procedure established in [15] is adapted and the bend angle is measured between a vertical line and straight line extending from the base to the center of the tip of the actuator. The results are shown in Fig. 6. Bending angles can also be measured with respect to the arc shape of the pressurised actuator, as described in [10], [24], [25], consequently all angles measured here would be multiplied by a factor of 2. As shown in Fig. 6, some actuators had a small initial curvature as a result of the manufacturing process, especially fiber wrapping, which is responsible for the bending offset at low pressures.

The actuators with no fiber wrapping (actuators 5, 13 and 15) exhibited a balloon effect, i.e. high radial expansion, which resulted in lower bending (bending angles below 50°). In fact, for pressures below approximately 50 kPa, all energy was spent in expanding the walls of the actuator and no bending initially occurred. The addition of fiber reinforcements has enhanced the respective extension or bending strokes of the actuators as it allows the use of higher pressure levels and minimises the energy lost in radial expansion of the rubber. Furthermore, for the fiber-reinforced bi-directional actuators (17 and 18), a higher density of wrapping (∼2 mm spacing between threads in actuator 17 in comparison to ∼5 mm in actuator 18) resulted in approximately 30% higher bending levels. A similar trend is also expected for the other actuators. In contrast, the normally undesired balloon behaviour can be explored to obtain anchoring or blocking segments for soft robots moving in tube-like environments.

Semi-circular actuators have shown the highest amount of bending. Indeed, with this cross-section, the addition of a fabric layer was not required for bending and did not show significant improvement in the bending stroke. Furthermore, lower wall thickness (1 mm in actuator 11 compared to 2 mm in actuator 12) has resulted in 60% higher bending. Finally, actuators fabricated with softer elastomer (DS10), such as actuators 10 and 14, have exhibited high levels of bending at even smaller input pressures. The highest bending angle

(115°) in this study is a result of blocking in the mechanical fixture (tip of the actuator comes in contact with the fixture) and further increase in the pressure would result in higher bending angles in a free space. In fact, by simply holding the bottom of actuators 10, 11 and 14 and applying pressure, these actuators curled around themselves (bending angles larger than 180°).

A popular design for soft actuator is the Parallel Bellows Actuator (PBA). It draws inspiration from the flexible microactuator developed by Suzumori et al. [29], [30] and is widely explored in pneumatic continuum robots [31]–[33]. PBA's can be manufactured by combining three extending actuators in a triangular pattern. When three chambers are actuated with the same pressure, the PBA stretches. In contrast, when only one or two chambers are actuated, the PBA bends in the direction opposite to the pressurised chambers. In this unconstrained configuration, a maximum bending angle of 45° was observed. By constraining the three extending actuators with rubber bands at the upper and lower sections, the maximum bending angle increased to 85°.

C. Twisting actuators

Measurements of twisting are difficult to obtain due to the combined extension or bending associated with these actuators. Possible experimental platforms for twisting characterisation consist of electromagnetic tracking or using two or more cameras placed at right angles and post-processing the images. By visual inspection of black lines marked on the tip of the fabricated twisting actuators, actuator 4 had a twisting angle of ∼45° at ∼400 kPa, actuator 9 showed ∼120° at ∼150 kPa, and actuator 19 had ∼70° at ∼80 kPa.

IV. CASE STUDY

A combination of the soft actuators previously discussed can be explored to achieve a variety of tasks. In this work, a worm-like soft robot whose motion mimics the peristaltic crawling of earthworms [34] to climb a pipe is introduced. In earthworms, longitudinal muscles are contracted in the anchoring segments, while circumferential muscles are contracted in the advancing segments [35], [36]. Given the previous discussion, extending actuators were readily available. The balloon effect of pressurized actuators with no fiber wrapping observed in the previous section is explored for the anchoring segments. In particular, the different behaviours under pressure of the two elastomer types can be used so that expansion only occurs in selected areas of the actuator. For that aim, multi-material actuators were fabricated with the sides being composed of Dragon Skin 10 (greater expansion), while caps of Elastosil M4601 were added at the top and bottom of the actuators. Consequently, with the input of pressure via the syringe, the actuator shows large radial expansion and small axial extension, enabling the anchoring behaviour.

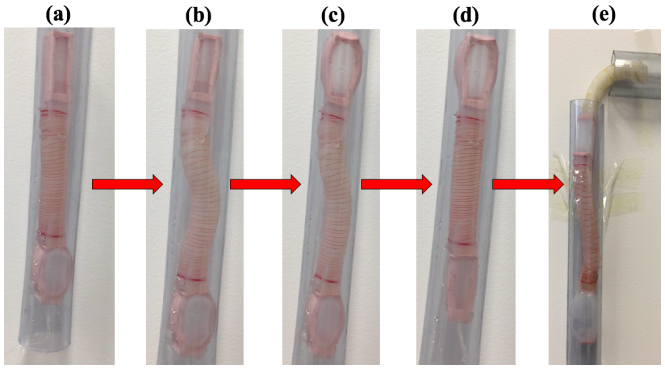

Fig. 7: Order of actuation for climbing a pipe. (a) Base actuator is pressurised to anchor the soft robot. (b) The extending actuator is pressurised. (c) Top actuator locks in position. (d) Base and extending actuators are depressurised. (e) Bending actuator at the tip is used for turning when a branching is reached.

In the fabrication of the soft robot, an extending actuator is glued to two of the newly developed multi-material actuators. The actuation of different segments of the soft robot, explained in Fig. 7, allows for the climbing motion. The tube selected in this study has a diameter of 32 mm, in contrast the actuators have sides between 15 mm and 20 mm, which exhibits the ability of these actuators to greatly expand without bursting.

Once the climbing motion is achieved, actuators can be added to achieve more complex trajectory matching. In this work, a semi-circular bending actuator is included at the tip of the previous soft robot to provide for branching selection. The soft robot is shown to be capable of turning 90° around a corner. This turning motion, however, was pre-selected and would not be achieved if the bending was required in another direction. Notice that addition of multiple bending segments or a twisting actuator in the base of the soft robot enables bending in different directions.

V. CONCLUSIONS

Soft fluidic actuators allow for a range of different motions by varying the geometry or materials selection. The addition of a strain limiting layer allows for bending and fiber reinforcements can be used to achieve twisting or higher levels of extension. By comparing actuators of the same length and similar thicknesses, semi-circular actuators are optimal shapes for bending and cylindrical actuators provide the best extension and twisting behaviours. The two determining factors in the actuator motion are the type of elastomer and the wrapping of fiber, with lower spacing between threads allowing for a higher stroke. Indeed, soft actuators fabricated using Dragon Skin 10 have shown higher levels of extension and bending at lower pressure levels (below 200 kPa) compared to M4601 actuators, a desired feature

for safe application to biomedical devices. The disadvantage with using Dragon Skin 10 is the lower force at the tip since DS10 actuators support lower pressures.

The soft actuators explored here have high modularity and can be used to achieve multiple motions and trajectory matching. As examples of this modularity, bi-directional and PBA actuators were manufactured and a bioinspired climbing motion was reproduced in a tube-like environment. However, with this approach, every actuator requires a drive line, which is a hindrance if miniaturisation and cost are considered. Future challenges include exploring the dynamics of actuation in order to minimise the amount of required drive lines; miniaturisation of soft actuators for medical applications; and investigation of alternative climbing strategies.

ACKNOWLEDGMENT

The authors would like to thank Phillip Dombkins and Priscilla Tan for the support with 3D printing.

REFERENCES

[1] M. Spong, S. Hutchinson, and M. Vidyasagar, *Robot Modeling and Control*. Wiley, 2005.

[2] M. Hannan and I. Walker, "Kinematics and the implementation of an elephant's trunk manipulator and other continuum style robots," *Journal of Robotic Systems*, vol. 20, no. 2, pp. 45–63, 2003.

[3] G. Robinson and J. Davies, "Continuum robots - a state of the art," in *Proceedings - IEEE International Conference on Robotics and Automation*, vol. 4, 1999, pp. 2849–2854.

[4] I. D. Walker, "Continuous backbone "continuum" robot manipulators," *ISRN robotics*, vol. 2013, 2013.

[5] R. Webster III and B. Jones, "Design and kinematic modeling of constant curvature continuum robots: A review," *International Journal of Robotics Research*, vol. 29, no. 13, pp. 1661–1683, 2010.

[6] D. Drotman, M. Ishida, S. Jadhav, and M. Tolley, "Application-driven design of soft, 3-d printed, pneumatic actuators with bellows," *IEEE/ASME Transactions on Mechatronics*, vol. 24, no. 1, pp. 78–87, 2019.

[7] L. Hines, K. Petersen, G. Lum, and M. Sitti, "Soft actuators for small-scale robotics," *Advanced Materials*, vol. 29, no. 13, 2017.

[8] D. Trivedi, C. Rahn, W. Kier, and I. Walker, "Soft robotics: Biological inspiration, state of the art, and future research," *Applied Bionics and Biomechanics*, vol. 5, no. 3, pp. 99–117, 2008.

[9] D. Rus and M. Tolley, "Design, fabrication and control of soft robots," *Nature*, vol. 521, no. 7553, pp. 467–475, 2015.

[10] P. Polygerinos, Z. Wang, J. Overvelde, K. Galloway, R. Wood, K. Bertoldi, and C. Walsh, "Modeling of soft fiber-reinforced bending actuators," *IEEE Transactions on Robotics*, vol. 31, no. 3, pp. 778–789, 2015.

[11] A. De Greef, P. Lambert, and A. Delchambre, "Towards flexible medical instruments: Review of flexible fluidic actuators," *Precision Engineering*, vol. 33, no. 4, pp. 311–321, 2009.

[12] B. Gorissen, M. De Volder, A. De Greef, and D. Reynaerts, "Theoretical and experimental analysis of pneumatic balloon microactuators," *Sensors and Actuators, A: Physical*, vol. 168, no. 1, pp. 58–65, 2011.

[13] B. Gorissen, D. Reynaerts, S. Konishi, K. Yoshida, J.-W. Kim, and M. De Volder, "Elastic inflatable actuators for soft robotic applications," *Advanced Materials*, vol. 29, no. 43, 2017.

[14] S. Konishi, F. Kawai, and P. Cusin, "Thin flexible end-effector using pneumatic balloon actuator," *Sensors and Actuators, A: Physical*, vol. 89, no. 1-2, pp. 28–35, 2001.

[15] Y. Hwang, O. Paydar, and R. Candler, "Pneumatic microfinger with balloon fins for linear motion using 3d printed molds," *Sensors and Actuators, A: Physical*, vol. 234, pp. 65–71, 2015.

[16] R. Shepherd, F. Ilievski, W. Choi, S. Morin, A. Stokes, A. Mazzeo, X. Chen, M. Wang, and G. Whitesides, "Multigait soft robot," *Proceedings of the National Academy of Sciences of the United States of America*, vol. 108, no. 51, pp. 20 400–20 403, 2011.

[17] B. Mosadegh, P. Polygerinos, C. Keplinger, S. Wennstedt, R. Shepherd, U. Gupta, J. Shim, K. Bertoldi, C. Walsh, and G. Whitesides, "Pneumatic networks for soft robotics that actuate rapidly," *Advanced Functional Materials*, vol. 24, no. 15, pp. 2163–2170, 2014.

[18] P. Polygerinos, S. Lyne, Z. Wang, L. Nicolini, B. Mosadegh, G. Whitesides, and C. Walsh, "Towards a soft pneumatic glove for hand rehabilitation," in *Proceedings - IEEE International Conference on Intelligent Robots and Systems*, 2013, pp. 1512–1517.

[19] Y. Sun, Y. Song, and J. Paik, "Characterization of silicone rubber based soft pneumatic actuators," in *Proceedings - IEEE International Conference on Intelligent Robots and Systems*, 2013, pp. 4446–4453.

[20] H.-W. Kang, I. Lee, and D.-W. Cho, "Development of a micro-bellows actuator using micro-stereolithography technology," *Microelectronic Engineering*, vol. 83, no. 4-9 SPEC. ISS., pp. 1201–1204, 2006.

[21] A. Marchese, R. Katzschmann, and D. Rus, "A recipe for soft fluidic elastomer robots," *Soft Robotics*, vol. 2, no. 1, pp. 7–25, 2015.

[22] T. Wallin, J. Pikul, and R. Shepherd, "3d printing of soft robotic systems," *Nature Reviews Materials*, vol. 3, no. 6, pp. 84–100, 2018.

[23] J. Gul, M. Sajid, M. Rehman, G. Siddiqui, I. Shah, K.-H. Kim, J.-W. Lee, and K. Choi, "3d printing for soft robotics–a review," *Science and Technology of Advanced Materials*, vol. 19, no. 1, pp. 243–262, 2018.

[24] K. Galloway, P. Polygerinos, C. Walsh, and R. Wood, "Mechanically programmable bend radius for fiber-reinforced soft actuators," in *Proceedings - International Conference on Advanced Robotics*, 2013.

[25] F. Connolly, C. Walsh, and K. Bertoldi, "Automatic design of fiber-reinforced soft actuators for trajectory matching," *Proceedings of the National Academy of Sciences of the United States of America*, vol. 114, no. 1, pp. 51–56, 2017.

[26] Y. Fu, H. Liu, W. Huang, S. Wang, and Z. Liang, "Steerable catheters in minimally invasive vascular surgery," *International Journal of Medical Robotics and Computer Assisted Surgery*, vol. 5, no. 4, pp. 381–391, 2009.

[27] X. Hu, A. Chen, Y. Luo, C. Zhang, and E. Zhang, "Steerable catheters for minimally invasive surgery: a review and future directions," *Computer Assisted Surgery*, vol. 23, no. 1, pp. 21–41, 2018.

[28] "Soft robotics toolkit," 2019, retrieved on 27/03/2019. [Online]. Available: https://softroboticstoolkit.com/components

[29] K. Suzumori, S. Iikura, and H. Tanaka, "Flexible microactuator for miniature robots," in *Proceedings - IEEE Micro Electro Mechanical Systems*, 1991, pp. 204–209.

[30] ——, "Development of flexible microactuator and its applications to robotic mechanisms," in *Proceedings - IEEE International Conference on Robotics and Automation*, vol. 2, 1991, pp. 1622–1627.

[31] W. McMahan, B. Jones, and I. Walker, "Design and implementation of a multi-section continuum robot: Air-octor," in *Proceedings - IEEE International Conference on Intelligent Robots and Systems*, 2005, pp. 3345–3352.

[32] W. McMahan, V. Chitrakaran, M. Csencsits, D. Dawson, I. Walker, B. Jones, M. Pritts, D. Dienno, M. Grissom, and C. Rahn, "Field trials and testing of the octarm continuum manipulator," in *Proceedings - IEEE International Conference on Robotics and Automation*, vol. 2006, 2006, pp. 2336–2341.

[33] S. Neppalli and B. Jones, "Design, construction, and analysis of a continuum robot," in *Proceedings - IEEE International Conference on Intelligent Robots and Systems*, 2007, pp. 1503–1507.

[34] M. Calisti, G. Picardi, and C. Laschi, "Fundamentals of soft robot locomotion," *Journal of the Royal Society Interface*, vol. 14, no. 130, 2017.

[35] K. Quillin, "Kinematic scaling of locomotion by hydrostatic animals: Ontogeny of peristaltic crawling by the earthworm lumbricus terrestris," *Journal of Experimental Biology*, vol. 202, no. 6, pp. 661–674, 1999.

[36] F. Connolly, P. Polygerinos, C. Walsh, and K. Bertoldi, "Mechanical programming of soft actuators by varying fiber angle," *Soft Robotics*, vol. 2, no. 1, pp. 26–32, 2015.